

## Supplementary Materials for A Crucial Role for RACK1 in the Regulation of Glucose-Stimulated IRE1 $\alpha$ Activation in Pancreatic $\beta$ Cells

Yifu Qiu, Ting Mao, Yongliang Zhang, Mengle Shao, Jia You, Qiurong Ding, Yan Chen,  
Dongmei Wu, Dong Xie, Xu Lin, Xiang Gao, Randal J. Kaufman, Wenjun Li,\*  
Yong Liu\*

\*To whom correspondence should be addressed. E-mail: liuy@sibs.ac.cn (Y.L.) and wjli@sibs.ac.cn  
(W.L.)

Published 26 January 2010, *Sci. Signal.* **3**, ra7 (2010)  
DOI: 10.1126/scisignal.2000514

### This PDF file includes:

#### Materials and Methods

Fig. S1. RACK1 associates with IRE1 $\alpha$  in transfected HEK 293T cells.

Fig. S2. High glucose stimulation does not trigger typical ER stress-activated UPR pathways.

Fig. S3. Glucose-stimulated phosphorylation does not cause an electrophoretic shift of the IRE1 $\alpha$  protein.

Fig. S4. Palmitate and insulin do not affect IRE1 $\alpha$  phosphorylation.

Fig. S5. Glucose metabolism and intracellular calcium mobilization are required for glucose stimulation of IRE1 $\alpha$  phosphorylation and IRE1 $\alpha$ -RACK1 interaction in  $\beta$  cells.

Fig. S6. The structural requirements for the interaction of IRE1 $\alpha$  with RACK1.

Fig. S7. Physical IRE1 $\alpha$ -RACK1 interaction requires the linker region of IRE1 $\alpha$ .

Fig. S8. Effects of RACK1 on ER stress-induced IRE1 $\alpha$  phosphorylation and *Xbp1* splicing in  $\beta$  cells.

Fig. S9. Prolonged exposure to high glucose, like ER stress, reduces the abundance of *Insulin* mRNA in  $\beta$  cells.

Fig. S10. Quantification of IRE1 $\alpha$  phosphorylation in INS-1 cells and primary islets.

Fig. S11. Autophosphorylation of overexpressed IRE1 $\alpha$ , RACK1 overexpression, or RACK1 knockdown does not affect *Insulin* mRNA abundance in INS-1  $\beta$  cells.

Fig. S12. Effects of adenoviral overexpression of IRE1 $\alpha$  or RACK1 or knockdown of RACK1 on glucose-stimulated insulin secretion in INS-1  $\beta$  cells.

Fig. S13. Decreased *Rack1* mRNA abundance and the effect of RACK1 overexpression on *Insulin* mRNA abundance in islets from *db/db* mice.

Fig. S14. Increased IRE1 $\alpha$  phosphorylation, decreased RACK1 abundance, and enhanced activation of the IRE1 $\alpha$  arm of the UPR in *db/db* islets.

Fig. S15. Analysis of the effect of adenoviral infections on the viability of INS-1  $\beta$  cells.

References

## **Materials and Methods**

### **Crystal violet assay**

INS-1 cells were seeded at equivalent densities in 12-well plates and infected for 48 hours with Ad-GFP or for 72 hours with Ad-shNC, or left uninfected. Cells were subsequently washed once with phosphate-buffered saline (PBS) and then incubated with 0.5% crystal violet solution in 20% methanol for 5 min at 37°C. After washing 8 times with PBS, cells were solubilized with 1% SDS and the absorbance at 595 nm was measured using a microplate reader.

### **MTT assay**

INS-1 cells were seeded at equivalent densities in 96-well plates and infected with Ad-GFP for 48 hours or Ad-shNC for 72 hours, or left uninfected. After adding 0.5 mg/ml MTT (Roche Applied Science) into the medium, cells were incubated in a 5% CO<sub>2</sub> incubator at 37°C for 2 hours. After removal of medium, 200 µl of DMSO was added into each well to dissolve the crystals for 5 minute at 37°C before the absorbance at 550 nm was measured using a microplate reader.

### **Measurement of adenoviral infection efficiency for primary islets**

Islets from 6 male C57 BL/6 mice at 14 weeks of age were pooled and infected with Ad-GFP at an MOI of 100 (with assumption of 2500 cells/islet) for 16 hours. Islets were then incubated with 0.0083% trypsin for 10 min at 37 °C with 5% CO<sub>2</sub>, and cells were dispersed by aspirating 5 times through an 18-gauge needle. Dispersed single cells were subsequently plated and cultured for 2 days before analysis for GFP-positive cells by fluorescent microscopy.

### **Oligonucleotide primers**

For regular RT-PCR:

rat *Xbp1*, forward primer 5'-AGCAAGTGGTGGATTTGGAAGAAG-3' and reverse primer 5'-AGGGTCCAACCTTGTCAGAAATG-3' (note that the 346-bp and 320-bp products correspond to the unspliced and spliced *Xbp1* mRNA, respectively).

For quantitative real-time RT-PCR:

rat *Bip*, forward primer 5'-AGAAGGTCACCCATGCAGTTG-3' and reverse primer 5'-GGCTCATTGATGATCCTCATG-3';

rat *Edem*, forward primer 5'-GCAATGAAGGAGAAGGAGAC-3' and reverse primer 5'-CCATATGGCATAGTAGAAGGC-3' (1);

rat *Chop*, forward primer 5'-GAAAGCAGAAACCGGTCCAAT-3' and reverse primer 5'-GGATGAGATATAGGTGCCCCC-3' (2);

rat *Insulin1*, forward primer 5'-GCCCAGGCTTTTGTCAAACA-3' and reverse primer 5'-CGGGACTTGGGTGTGTAGAAG-3';

rat *Insulin2*, forward primer 5'-GGTTCTCACTTGGTGGGAAGCTC-3' and reverse primer 5'-GTGCCAAGGTCTGAAGGTCAC-3';

rat *Gapdh*, forward primer 5'-GGATTTGGCCGTATCGG-3' and reverse primer 5'-GTTGAGGTCAATGAAGGGG-3';

mouse *Insulin1*, forward primer 5'-TCTTCTACACACCCAAGTCCCG-3' and reverse primer 5'-CTCCAACGCCAAGGTCTGAA-3';

mouse *Insulin2*, forward primer 5'-CTTCTTCTACACACCCATGTCCC-3' and reverse primer 5'-CCAAGGTCTGAAGGTCACCTG-3';

mouse *Rack1*, forward primer 5'-TTCTCCTCTGACAACCGGCA-3' and reverse primer 5'-GCCATCCTTGCCCTCCAGAA-3' (also used for rat *Rack1* by regular RT-PCR);

mouse *sXbp1*, forward primer 5'-CTGAGTCCGAATCAGGTGCAG-3' and reverse primer 5'-GTCCATGGGAAGATGTTCTGG-3' (3);

mouse *Edem*, forward primer 5'-AAGCCCTCTGGAAGTTGCG-3' and reverse primer 5'-AACCCAATGGCCTGTCTGG-3' (4);

mouse *ERdj4*, forward primer 5'-CCCCAGTGTCAAAGTGTACCAG-3' and reverse primer 5'-AGCGTTTCCAATTTTCCATAAATT-3'(4);

mouse *Gapdh*, forward primer 5'-GGATTTGGCCGTATTGGG-3' and reverse primer 5'-GTTGAGGTCAATGAAGGGG-3',

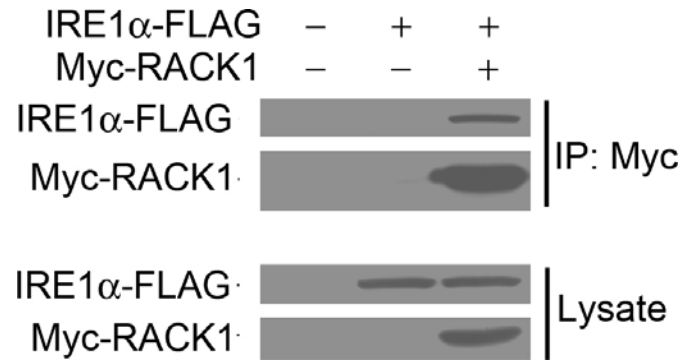


**Fig. S1. RACK1 associates with IRE1 $\alpha$  in transfected HEK 293T cells.**

HEK 293T cells were transfected for 48 hours with empty vector or the plasmid encoding FLAG-tagged human IRE1 $\alpha$ , or cotransfected with FLAG-tagged IRE1 $\alpha$  and Myc-tagged human RACK1. Cell lysates were immunoprecipitated with antibody against Myc. Immunoblotting was conducted with antibodies against FLAG and Myc. Results are representative of two independent experiments.

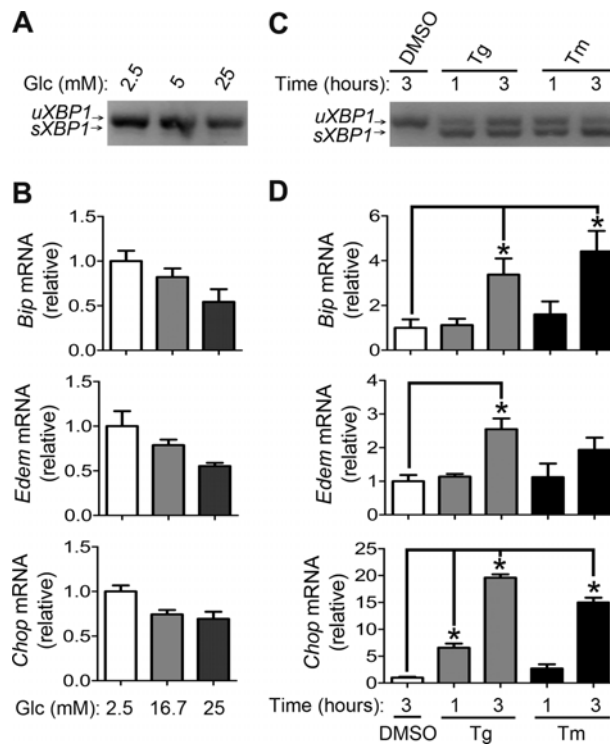


**Fig. S2. High glucose stimulation does not trigger typical ER stress-activated UPR pathways.**

(A and B) INS-1  $\beta$ -cells maintained in 5 mM glucose for 18 hours were cultured for 3 hours in medium with glucose at 2.5, 16.7, or 25 mM. (C and D) INS-1  $\beta$ -cells cultured in 5 mM glucose for 18 hours were treated with DMSO, thapsigargin (Tg, 2  $\mu$ M), or tunicamycin (Tm, 10  $\mu$ g/ml) for 1 or 3 hours. (A and C) The mRNA abundance of spliced (s) and unspliced (u) *Xbp1* was analyzed by RT-PCR. Results are representative of three independent experiments. (B and D) The mRNA abundance of known UPR target genes (*Bip*, *Edem*, and *Chop*) was analyzed by quantitative real-time RT-PCR. Data are shown as mean values  $\pm$  SEM (n=3 independent experiments). \*P<0.05 compared to DMSO by one-way ANOVA.

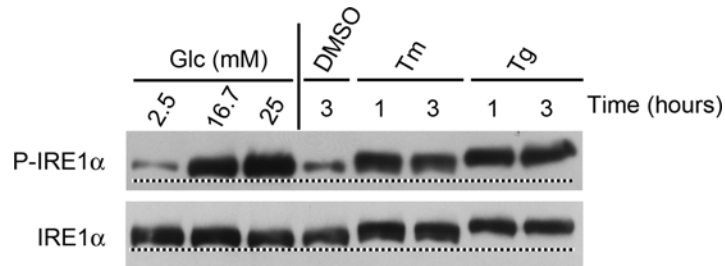


**Fig. S3. Glucose-stimulated phosphorylation does not cause an electrophoretic shift of the IRE1 $\alpha$  protein.**

INS-1  $\beta$ -cells maintained in 5 mM glucose for 18 hours were cultured for 3 hours in medium with glucose at 2.5, 16.7, or 25 mM, or treated with DMSO, thapsigargin (Tg, 2  $\mu$ M), or tunicamycin (Tm, 10  $\mu$ g/ml) for 1 or 3 hours. Cell lysates were subjected to analysis by 7% SDS-PAGE, and immunoblotting was conducted using antibodies against IRE1 $\alpha$  [pSer<sup>724</sup>] and IRE1 $\alpha$ , respectively. Results are representative of three independent experiments.



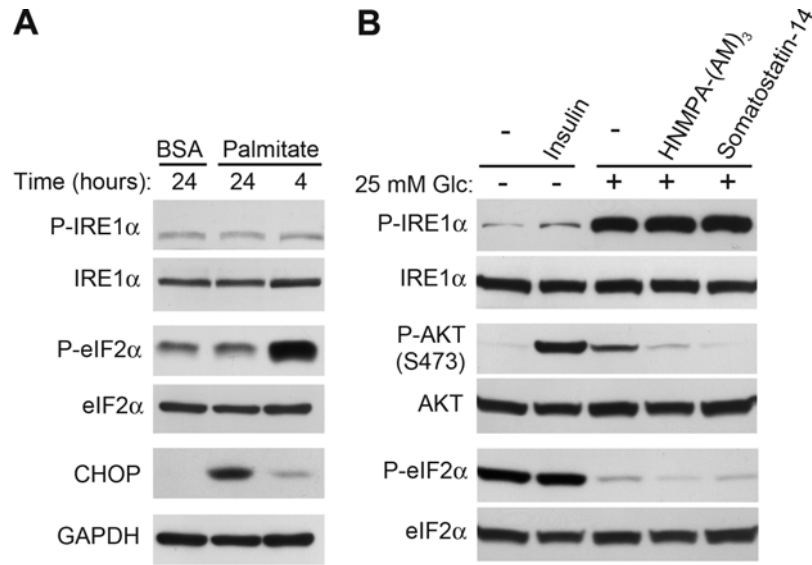


**Fig. S4. Palmitate and insulin do not affect IRE1 $\alpha$  phosphorylation.**

(A) INS-1  $\beta$ -cells maintained in 5 mM glucose for 18 hours were cultured in the presence of 0.4 mM palmitate and 0.4% BSA or 0.4% BSA for the indicated time intervals. (B) INS-1  $\beta$ -cells maintained in 5 mM glucose without serum for 14 hours were cultured in medium without glucose for 4 hours. Cells were then cultured for 3 hours in serum-free medium with 100 nM insulin, or with 25 mM glucose in the absence or presence of 10  $\mu$ M HNMPA-(AM)<sub>3</sub> (an inhibitor of insulin receptor tyrosine kinase activity) (5, 6), or 500 nM somatostatin-14 (an inhibitor of insulin secretion) (7). Cell lysates were analyzed by immunoblotting with the indicated antibodies. Shown are representative results of three independent experiments.

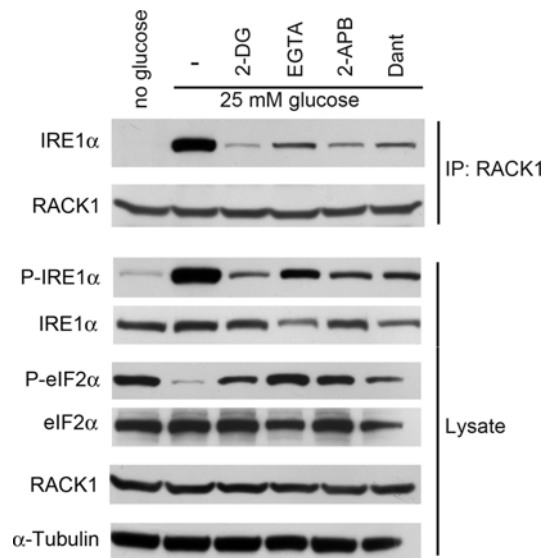


**Fig. S5. Glucose metabolism and intracellular calcium mobilization are required for glucose stimulation of IRE1 $\alpha$  phosphorylation and IRE1 $\alpha$ -RACK1 interaction in  $\beta$ -cells.**

INS-1  $\beta$ -cells maintained in 5 mM glucose without serum for 14 hours were pre-cultured in serum-free medium without glucose for 4 hours. Cells were then cultured for 3 hours in 25 mM glucose in the absence or presence of 20 mM 2-deoxyglucose (2-DG, an inhibitor of glucose glycolysis) (8), or 5 mM EGTA (a blocker of calcium influx), or 50  $\mu$ M 2-APB (an inhibitor of ER calcium release through the IP<sub>3</sub> receptor) (9) or 50  $\mu$ M dantrolene (a blocker of ER calcium release through ryanodine receptors) (9). Immunoprecipitation was performed with anti-RACK1, and immunoblotting was conducted using the indicated antibodies. Results are representative of three independent experiments.

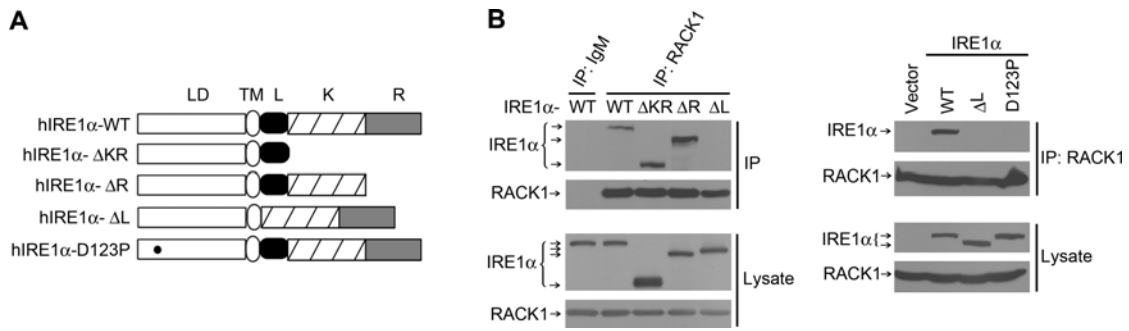


**Fig. S6. The structural requirements for the interaction of IRE1 $\alpha$  with RACK1.**

(A) Diagram of the wild type (WT) and mutant versions of FLAG-tagged IRE1 $\alpha$  analyzed. The luminal domain (LD), transmembrane segment (TM), linker region (L), kinase (K), and RNase (R) domains are indicated. (B) The IRE1 $\alpha$  linker region and dimerization are essential for interaction with RACK1. HEK 293T cells were transfected with plasmids encoding the WT, the indicated deletion mutants, or the dimerization-defective D123P mutant of IRE1 $\alpha$ . Immunoprecipitation was conducted using anti-RACK1, followed by immunoblotting with antibodies against RACK1, IRE1 $\alpha$ , or FLAG. Results are representative of two independent experiments.

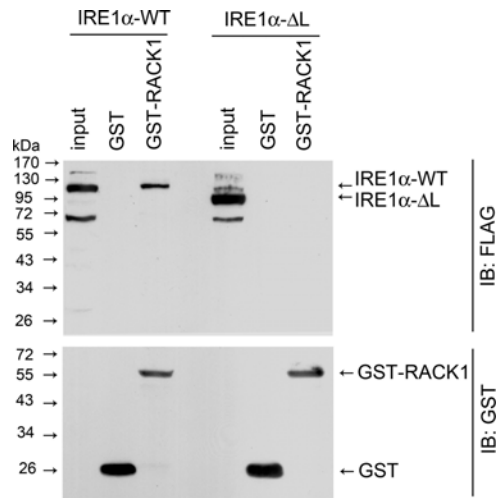


**Fig. S7. Physical IRE1 $\alpha$ -RACK1 interaction requires the linker region of IRE1 $\alpha$ .**

HEK 293T cells were transfected with plasmids encoding FLAG-tagged IRE1 $\alpha$ -WT or the IRE1 $\alpha$ - $\Delta$ L mutant. Forty-eight hours post-transfection, GST pull-down assays were performed by incubating cell lysates with Glutathione-Sepharose-4B beads and purified GST or GST-RACK1 fusion proteins expressed in *E. coli*. Fractions bound to the beads were subsequently analyzed by immunoblotting (IB) using the indicated antibodies.

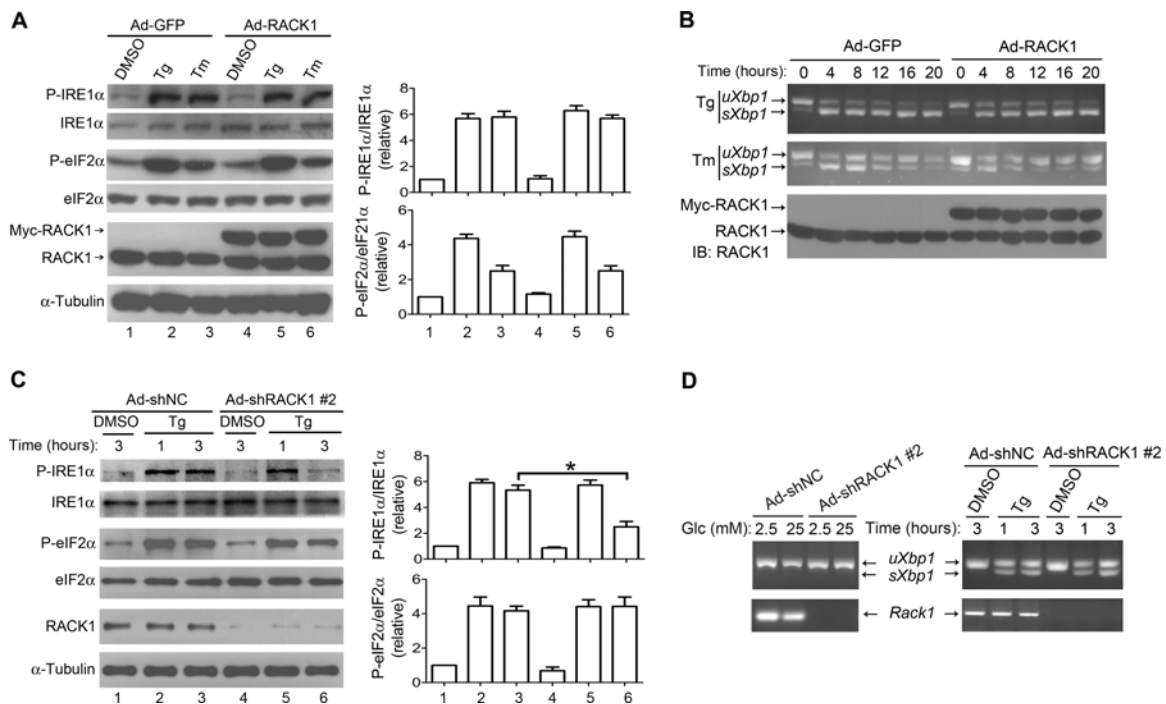


**Fig. S8. Effects of RACK1 on ER stress-induced IRE1 $\alpha$  phosphorylation and *Xbp1* splicing in  $\beta$ -cells.**

(A and B) Overexpression of RACK1 does not affect ER stress-induced IRE1 $\alpha$  phosphorylation or *Xbp1* splicing in  $\beta$ -cells. INS-1 cells were infected at an MOI of 10 for 48 hours with recombinant adenoviruses expressing GFP or Myc-tagged RACK1. Infected cells maintained in 5 mM glucose for 18 hours were treated with DMSO, thapsigargin (Tg, 2  $\mu$ M), or tunicamycin (Tm, 10  $\mu$ g/ml) for 3 hours (A) or the indicated time intervals (B). (C and D) RACK1 knockdown does not increase ER stress-induced IRE1 $\alpha$  phosphorylation or affect *Xbp1* mRNA splicing in  $\beta$ -cells. INS-1 cells were infected at an MOI of 40 for 72 hours with adenoviruses Ad-shNC or Ad-shRACK1 #2. Cells were subsequently maintained in 5 mM glucose for 18 hours, and then incubated with 2.5 or 25 mM glucose for 3 hours or treated with DMSO or thapsigargin (Tg, 2  $\mu$ M) for 1 or 3 hours. In panels (A) and (C), the amount of P-IRE1 $\alpha$  to total IRE1 $\alpha$  as well as

that of P-eIF2 $\alpha$  to total eIF2 $\alpha$  was analyzed by immunoblotting using the indicated antibodies. RACK1 was detected with anti-RACK1. The fold changes of IRE1 $\alpha$  or eIF2 $\alpha$  phosphorylation were determined from densitometric quantifications and shown as means  $\pm$  SEM (n=3-4 independent experiments). \*P < 0.05 by two-way ANOVA. In panels (B) and (D), the mRNA abundance of spliced (s) or unspliced (u) *Xbp1* was analyzed by RT-PCR, and RACK1 was detected by (B) immunoblotting with anti-RACK1 or (D) RT-PCR analysis.

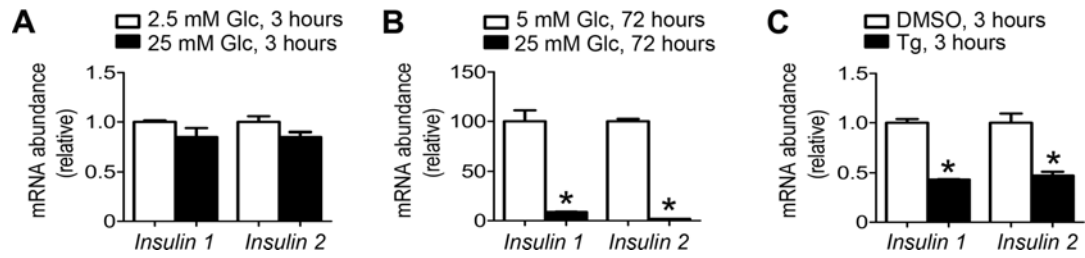


**Fig. S9. Prolonged exposure to high glucose, like ER stress, reduces the abundance of *Insulin* mRNA in  $\beta$ -cells.**

(A to C) INS-1  $\beta$ -cells maintained in 5 mM glucose were cultured in medium with glucose at 2.5 or 25 mM for (A) 3 hours or (B) 72 hours, or (C) treated with DMSO or thapsigargin (Tg, 2  $\mu$ M) for 3 hours. The mRNA abundance of *Insulin 1* or *Insulin 2* was analyzed by quantitative real-time RT-PCR. Data are shown as means  $\pm$  SEM (n=3 independent experiments). \*P < 0.05 by unpaired two-tailed *t*-test.

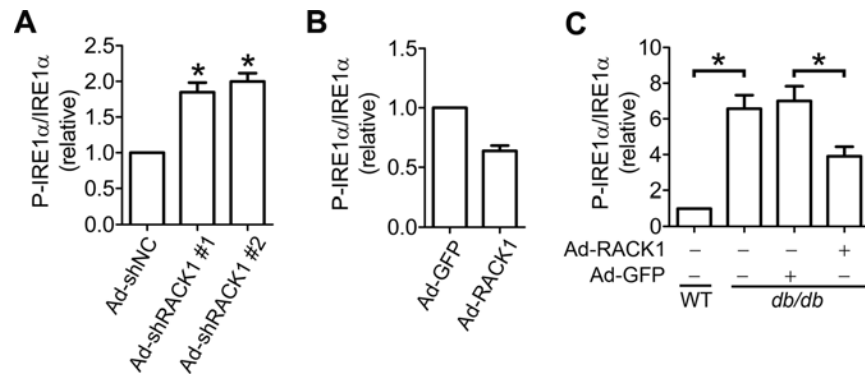


**Fig. S10. Quantification of IRE1 $\alpha$  phosphorylation in INS-1 cells and primary islets.**

(A to C) Relative ratios of P-IRE1 $\alpha$  normalized to total IRE1 $\alpha$  were determined by densitometric quantitation of immunoblots of (A) RACK1 knockdown INS-1 cells, \*P<0.05 by one-way ANOVA, (B) islets infected by Ad-GFP or Ad-RACK1, and (C) the islets from *db/db* mice as shown in Fig. 5B, 5C and 5D, respectively. All values are presented as means  $\pm$  SEM (n=3 independent experiments). \*P<0.05 by unpaired two-tailed *t*-test.



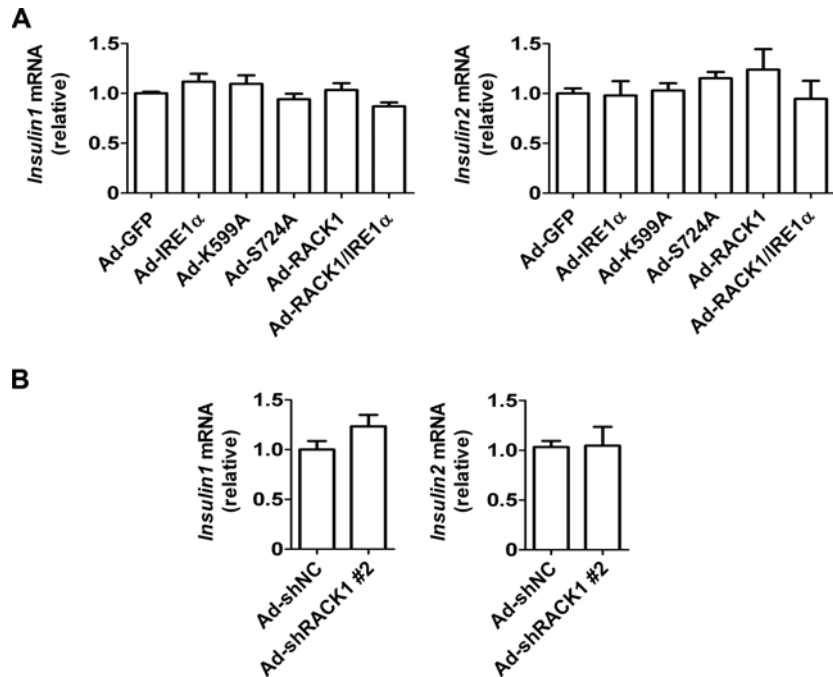


**Fig. S11. Autophosphorylation of overexpressed IRE1 $\alpha$ , RACK1 overexpression, or RACK1 knockdown does not affect *Insulin* mRNA abundance in INS-1  $\beta$ -cells.**

(A) INS-1 cells maintained in 11.1 mM glucose were infected with control adenovirus Ad-GFP (at an MOI of 20), or co-infected for 48 hours at a total MOI of 20 with Ad-GFP (at an MOI of 10) and viruses expressing the indicated forms of IRE1 $\alpha$  or Ad-RACK1, or Ad-IRE1 $\alpha$ -WT with Ad-RACK1. (B) INS-1 cells cultured in 11.1 mM glucose were infected with adenoviruses Ad-shNC or Ad-shRACK1 #2 for 72 hours. Total cellular RNA was isolated, and the mRNA abundance of *Insulin 1* or *Insulin 2* were determined by quantitative real-time RT-PCR. Values are shown as means  $\pm$  SEM from three independent experiments after normalization to *Gapdh* as an internal control. Analysis by one-way ANOVA (A) or unpaired two-tailed *t*-test (B) indicates no statistical significance between different groups.

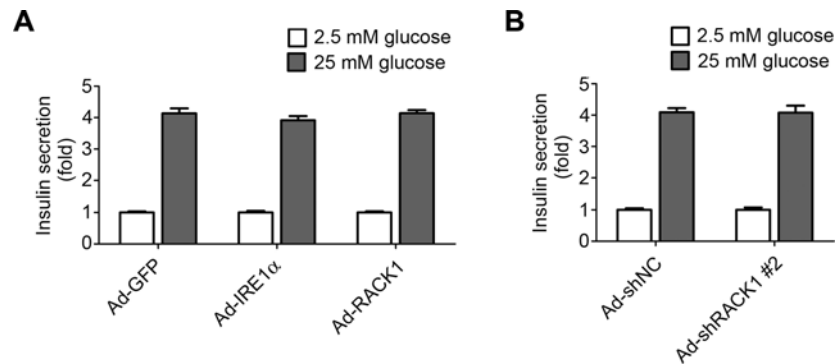


**Fig. S12. Effects of adenoviral overexpression of IRE1 $\alpha$  or RACK1 or knockdown of RACK1 on glucose-stimulated insulin secretion in INS-1  $\beta$ -cells.**

(A) INS-1 cells maintained in 11.1 mM glucose were infected with recombinant adenoviruses encoding GFP, IRE1 $\alpha$ , or RACK1 for 48 hours. (B) INS-1 cells were infected with adenoviruses Ad-shNC or Ad-shRACK1 #2 for 72 hours. Cells were subsequently incubated in 2.5 mM or 25 mM glucose for 2 hours, and secreted insulin was measured using a radioimmunoassay kit. Shown are fold increases in glucose-stimulated insulin secretion relative to basal amounts in 2.5 mM glucose. Data are presented as means  $\pm$  SEM from four independent experiments. Two-way ANOVA analysis indicates no statistical significance between different groups.

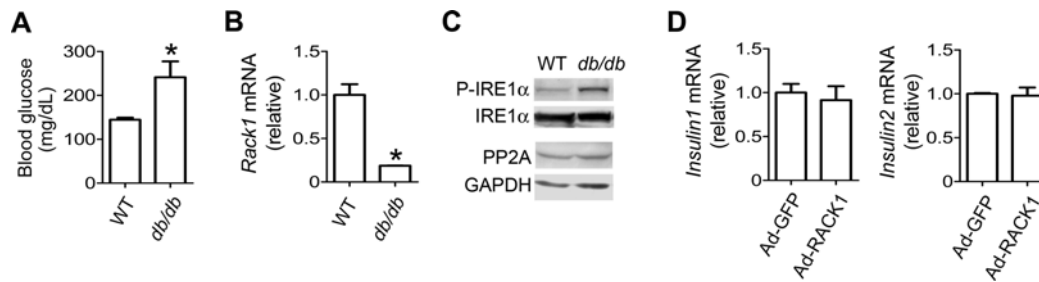


**Fig. S13. Decreased *Rack1* mRNA abundance and the effect of RACK1 overexpression on *Insulin* mRNA abundance in the islets of *db/db* mice.**

(A) Blood glucose concentrations were determined after a 16-hour fast in 14-week old male *db/db* mice and their wild-type (WT) littermates in the C57BL/6 background. Values are shown as means  $\pm$  SEM (n=7-10 mice per group). \*P < 0.05 compared to WT by unpaired two-tailed *t*-test. (B to D) Primary islets were isolated and pooled from 6-7 male *db/db* mice or 7-10 WT littermates at 14-16 weeks of age. (B) The mRNA abundance of *Rack1* was determined by quantitative real-time RT-PCR, and are shown as means  $\pm$  SEM after normalization to *Gapdh* as an internal control (n=3 independent experiments). \*P < 0.05 compared WT by unpaired two-tailed *t*-test. (C) PP2A protein abundance and IRE1 $\alpha$  phosphorylation were assessed by immunoblotting with the indicated antibodies. (D) Islets pooled from *db/db* mice were infected with adenoviruses expressing GFP or RACK1 for 48 hours. The mRNA abundance of *Insulin 1* or *Insulin 2* was analyzed by quantitative RT-PCR using total islet RNA. Values are shown as means  $\pm$  SEM after normalization to *Gapdh* as an internal control (n=3 independent experiments). Analysis by unpaired two-tailed *t*-test indicates no statistical significance between different groups.

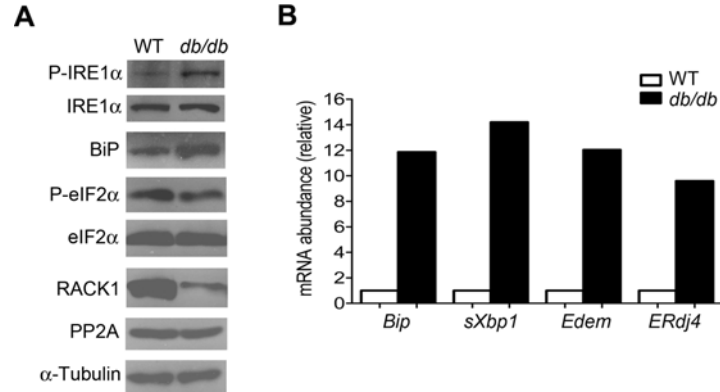


**Fig. S14. Increased IRE1 $\alpha$  phosphorylation, decreased RACK1 abundance, and enhanced activation of the IRE1 $\alpha$  arm of the UPR in *db/db* islets.**

Primary islets were isolated and pooled from 12 WT and 8 *db/db* mice at 15 weeks of age.

(A) Phosphorylation of IRE1 $\alpha$  or eIF2 $\alpha$  was analyzed by immunoblotting. (B) The mRNA abundance of *Bip*, the spliced form of *Xbp1* (*sXbp1*), and the XBP-1 target genes *Edem* and *ERdj4* were determined by quantitative real-time RT-PCR in triplicate. The fold changes in the abundance of each mRNA transcript in *db/db* mice relative to their wild-type littermates are shown after normalization to *Gapdh* as an internal control.

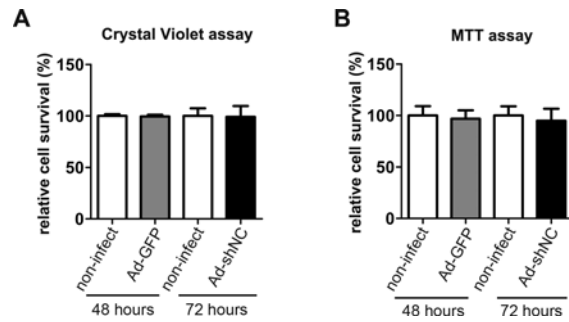


**Fig. S15. Analysis of the effects of adenoviral infections on the viability of INS-1  $\beta$ -cells.**

(**A** and **B**) INS-1 cells were infected with Ad-GFP at an MOI of 20 for 48 hours or left uninfected, or infected with Ad-shNC at an MOI of 40 for 72 hours or left uninfected. Cell viability was determined by (A) crystal violet or (B) MTT assay. Data are shown as the averaged cell survival count in percentage after normalization to the non-infection control which was set at 100 (n=3 independent experiments). Unpaired two-tailed *t*-test analysis indicates no statistical significance between different groups.

## References

1. M. J. Pagliassotti, Y. Wei, D. Wang, Insulin protects liver cells from saturated fatty acid-induced apoptosis via inhibition of c-Jun NH2 terminal kinase activity. *Endocrinology* **148**, 3338-3345 (2007).
2. B. L. Williams, W. I. Lipkin, Endoplasmic reticulum stress and neurodegeneration in rats neonatally infected with borna disease virus. *J Virol* **80**, 8613-8626 (2006).
3. K. L. Lipson, S. G. Fonseca, S. Ishigaki, L. X. Nguyen, E. Foss, R. Bortell, A. A. Rossini, F. Urano, Regulation of insulin biosynthesis in pancreatic beta cells by an endoplasmic reticulum-resident protein kinase IRE1. *Cell Metab* **4**, 245-254 (2006).
4. A. H. Lee, G. C. Chu, N. N. Iwakoshi, L. H. Glimcher, XBP-1 is required for biogenesis of cellular secretory machinery of exocrine glands. *EMBO J* **24**, 4368-4380 (2005).
5. R. Saperstein, P. P. Vicario, H. V. Strout, E. Brady, E. E. Slater, W. J. Greenlee, D. L. Ondeyka, A. A. Patchett, D. G. Hangauer, Design of a selective insulin receptor tyrosine kinase inhibitor and its effect on glucose uptake and metabolism in intact cells. *Biochemistry* **28**, 5694-5701 (1989).
6. L. E. Diaz, Y. C. Chuan, M. Lewitt, L. Fernandez-Perez, S. Carrasco-Rodriguez, M. Sanchez-Gomez, A. Flores-Morales, IGF-II regulates metastatic properties of choriocarcinoma cells through the activation of the insulin receptor. *Mol Hum Reprod* **13**, 567-576 (2007).
7. M. Z. Strowski, R. M. Parmar, A. D. Blake, J. M. Schaeffer, Somatostatin inhibits insulin and glucagon secretion via two receptors subtypes: an in vitro study of pancreatic islets from somatostatin receptor 2 knockout mice. *Endocrinology* **141**, 111-117 (2000).
8. G. E. Woodward, M. T. Hudson, The effect of 2-desoxy-D-glucose on glycolysis and respiration of tumor and normal tissues. *Cancer Res* **14**, 599-605 (1954).
9. D. Arnette, T. B. Gibson, M. C. Lawrence, B. January, S. Khoo, K. McGlynn, C. A. Vanderbilt, M. H. Cobb, Regulation of ERK1 and ERK2 by glucose and peptide hormones in pancreatic beta cells. *J Biol Chem* **278**, 32517-32525 (2003).